



## Analytical Methods

# An electrochemical aptasensor based on gold nanoparticles dotted graphene modified glassy carbon electrode for label-free detection of bisphenol A in milk samples

Ling Zhou<sup>a</sup>, Jianping Wang<sup>a,\*</sup>, Dujuan Li<sup>b</sup>, Yanbin Li<sup>a,c</sup><sup>a</sup> College of Biosystems Engineering and Food Science, Zhejiang University, Hangzhou 310058, China<sup>b</sup> College of Life Information Science and Instrument Engineering, Hangzhou Dianzi University, Hangzhou 310058, China<sup>c</sup> Department of Biological and Agricultural Engineering, University of Arkansas, Fayetteville, AR 72701, USA

## ARTICLE INFO

## Article history:

Received 17 November 2013

Received in revised form 28 March 2014

Accepted 13 April 2014

Available online 24 April 2014

## Keywords:

Electrochemical biosensor

Aptamer

Gold nanoparticles dotted graphene

Bisphenol A

## ABSTRACT

A simple and label-free electrochemical aptasensor for bisphenol A (BPA) determination was developed based on gold nanoparticles dotted graphene (GNPs/GR) nanocomposite film modified glassy carbon electrode (GCE). The electrochemical probe of ferricyanide was used to investigate the interactions between aptamer and BPA. The resulting GNPs/GR layer exhibited good current response for BPA detection. The highly conductive and biocompatible nanostructure of GNPs/GR nanocomposite was characterised by atomic force microscope (AFM), scanning electron microscopy (SEM) and cyclic voltammetry (CV). The peak current change ( $\Delta I$ ) of ferricyanide was linear with the concentration of BPA in the range from 0.01  $\mu\text{M}$  to 10  $\mu\text{M}$  with the detection limit of 5 nM. The proposed aptasensor is rapid, convenient and low-cost for effective sensing of BPA. Particularly, the aptasensor was applied successfully to determine BPA in milk products, and the average recovery was 105%.

© 2014 Elsevier Ltd. All rights reserved.

## 1. Introduction

Bisphenol A (BPA) is one of the endocrine disrupting compounds, which could mimic the action of hormone oestrogen and disturb the oestrogen–oestrogen receptor binding process of human and wildlife, increase cancer rate, decrease semen quality and reduce immune function (Hiroi et al., 1999 and Safe, 2000). However, BPA is an organic compound that widely used in the plastic industry as a monomer for producing epoxy resins and polycarbonate (Palanza, Gioiosa, vom Saal, & Parmigiani, 2008). The plastic products are extensively employed for nursing bottles, food can linings, beverage containers, from which BPA can permeate into food and environment, and thus humans may routinely ingest trace amounts of BPA (Le, Carlson, Chua, & Belcher, 2008 and Sato, Kondo, Tsujita, & Kawai, 2005). To protect water quality and human health, Chinese Health Standard (GB 13116-91, GB 14942-94) proposed that the BPA content of both carbonate resins and its derivatives should not be greater than

0.05 mg kg<sup>-1</sup>. Therefore, there is a great need to develop sensitive and reliable analytical method for the determination of BPA.

To date, many analytical technologies have been developed for BPA detection, such as high performance liquid chromatography (HPLC) (Inoue, Kato, Yoshimura, Makino, & Nzkazawa, 2000 and Watabe et al., 2004), liquid chromatography (LC) (Zafra-Gómez, Ballesteros, Navalón, & Vilchez, 2008), gas chromatography coupled with mass spectrometry (GC/MS) (Chanbasha & Lee, 2004) and immunoassay methods (Zhao, Li, Guo, Zhang, & Chang, 2002 and Moreno, D'Arienzo, Manclus, & Montoya, 2011). These instrument-based techniques have high sensitivity and low detection limit, but they are expensive, have strict sample preparation requirements and require trained operators. Immunoassay-based methods have also attracted considerable attention for BPA detection due to the high sensitivity and comparable low costs. However, they are strongly dependent on the quality of the prepared antibody, while there have been some reports about non-specific binding to the high structural similarity of BP derivatives, such as bisphenol B (BPB) and 4,4-bis-(4-hydroxyphenyl) valeric acid (Ohkuma et al., 2002 and Marchesini, Meulenberg, Haasnoot, & Irth, 2005). Furthermore, direct electrochemical methods have been applied to detect BPA for a long time (Wang, Yang, & Wu, 2009 and Yin et al., 2011). However, the fouling of electrode

\* Corresponding author. Address: College of Biosystems Engineering and Food Science, Zhejiang University, 866 Yuhangtang Road, Hangzhou 310058, China. Tel./fax: +86 571 88982350.

E-mail address: [jpwang@zju.edu.cn](mailto:jpwang@zju.edu.cn) (J. Wang).

surface by BPA oxidation product can result in poor performance at the conventional electrodes.

Aptamers are artificial, short, single-stranded DNA/RNA oligonucleotides that are selected *in vitro* by systematic evolution of ligands by exponential enrichment (SELEX) (Ellington & Szostak, 1990 and Tuerk & Gold, 1990). Aptamers can successively compete with antibodies as biorecognition elements for biosensors due to their specific properties. They can be selected to bind a wide range of targets, including small molecules, proteins or even whole cells with high specificity and affinity (Bang, Cho, & Kim, 2005; Huang, Huang, Cao, Tan, & Chang, 2005; Stojanovic & Landry, 2002 and Wilson & Szostak, 1999). They are thermally stable, reusable and can be easily modified for their detection and immobilisation by introducing of functional groups. Therefore, aptamer-based sensors have been broadly used in detection of cancer cells, organic molecules, and a variety of proteins. Among them, electrochemical aptamer-based sensors are widely employed due to their excellent sensitivity, rapid response, simplicity and low cost.

In order to enhance the sensitivity of the electrochemical aptasensors, a variety of materials have been employed to modify electrode. Graphene (GR) is a two-dimensional sheet of carbon atoms bonded through  $sp^2$  hybridisation. GR has attracted intensive interests in recent years since its discovery by Geim and coworkers, owing to its large specific area, high thermal and electrical conductivities, great mechanical strength, and potential low manufacturing cost (Al-Mashat et al., 2010 and Hong et al., 2010). Furthermore, gold nanoparticles dotted graphene (GNPs/GR) as enhanced sensing material for fabricating electrochemical sensors have received increased attention, because this kind of nanomaterial film may generate synergy on electrochemical properties and thus enhance the sensitivity of the sensors (Li, Xia, Li, Sun, & Liu, 2013).

In this work, we proposed a simple and sensitive electrochemical aptasensor for BPA determination based on good current response resulting from GNPs/GR nanocomposites. The anti-BPA aptamer was immobilised on a glassy carbon electrode through the formation of thiol–gold (S–Au) bonds between the gold nanoparticles and thiol termini on aptamers. The interaction between anti-BPA aptamer and target was investigated by the electrochemical probe of ferricyanide and monitored by cyclic voltammetry (CV) and differential pulse voltammetry (DPV). The SEM and electrochemical characterisation of the GNPs/GR and the performance of the resulted aptasensor were discussed as follows. Finally, the proposed aptasensor was applied to determine BPA in milk samples.

## 2. Experimental

### 2.1. Chemicals and reagents

The synthetic anti-BPA aptamer (sequence designed by Jo et al. (2011): 5'-SH-(CH<sub>2</sub>)<sub>6</sub>-CCG GTG G GT GGT CAG GTG GGA TAG CGT TCC GCG TAT GGC CCA GCG CAT CAC GGG TTC GC A CCA-3' was obtained from Sangon Biotechnology Co. Ltd. (Shanghai, China). Graphene Oxide (GO) was purchased from Nanjing Xianfeng Nano Co. Ltd. (Nanjing, China). 6-Mercapto-1-hexanol (MCH) and tris-(2-carboxyethyl) phosphine hydrochloride (TCEP) were obtained from Sigma–Aldrich (St. Louis, MO, USA). Chlorauric acid (HAuCl<sub>4</sub>) was purchased from Aladdin Reagent Co. Ltd. (Shanghai, China). Bisphenol A (BPA), bisphenol B, 6F bisphenol A, and 4,4'-biphenol (BP) were purchased from Sinopharm Chemical Reagent Co. Ltd. (Shanghai, China). All other reagents were of analytical grade and used without further purification. Ultrapure water obtained from a Millipore water purification system ( $\geq 18$  M  $\Omega$ , Milli-Q Millipore) was used in all assays and solutions.

### 2.2. Apparatus

Electrochemical measurements were carried out with a CHI 440A Electrochemical Workstation (Shanghai CH Instrument Inc., China). All experiments were carried out with a conventional three-electrode system with glassy carbon electrode (GCE) as the working electrode (WE), a platinum counter electrode (CE) and an Ag/AgCl (sat. KCl) reference electrode (RE). Scan electron microscopy (SEM) images were recorded using Philips XL30 scanning electron microscopy (Philips, Amsterdam, Dutch). The conditions used for SEM determination were set as follows: accelerating voltage, 20.0 kV; working distance, 3.0 mm; and coating Au. Atomic force microscopy (AFM) measurements were conducted on a Dimension Icon AFM equipped with a ScanAsyst (Bruker AXS, Karl Sruhe, Germany). The conditions used for AFM determination were set as follows: scan size, 3.0  $\mu\text{m}$ ; scan rate, 0.999 Hz.

### 2.3. Preparation of GNPs/GR based aptasensor

The fabrication of the aptasensor includes three steps as follows: the pretreatment of GCE, immobilisation of GNPs/GR nanocomposite film, and self-assembly of anti-BPA aptamer (Supplementary file, Scheme S1). Firstly, A GCE was polished on chamois leather with 1.0, 0.3, and 0.05  $\mu\text{m}$  Al<sub>2</sub>O<sub>3</sub> slurry successively followed by rinsing thoroughly with double-distilled water until a mirror-like surface was obtained. Then it was washed ultrasonically in absolute ethanol and double-distilled water for 5 min, respectively, and finally dried under a stream of nitrogen at room temperature.

On the second step, 5.0  $\mu\text{L}$  of 1.0  $\text{mg mL}^{-1}$  suspension of GO was dropped onto a freshly smoothed GCE surface uniformly, and the solvent was evaporated at room temperature. The prepared electrode was thoroughly rinsed with ultrapure water to remove excessive GO. Electrochemical reduction of GO on the electrode surface was performed in the N<sub>2</sub> purged PBS solution (pH 8.0) at a working potential of  $-1.2$  V (vs Ag/AgCl) for 1200 s. The modified electrode was then immersed in a 0.1 mM chlorauric acid solution containing 0.5 M sulphuric acid to electrodeposit GNPs with constant potential at  $-0.25$  V for 30 s. The electrode was rinsed with ultrapure water and allowed to dry at room temperature.

The last step is the self-assembly of anti-BPA aptamer (anti-BPA) onto the GNPs/GR modified GCE. Before use, the anti-BPA aptamer was firstly prepared as follows: the anti-BPA aptamer was denatured by heating at 90 °C for 10 min, quickly cooled at 4 °C for 15 min and incubated at 25 °C for 5 min to allow renaturation of aptamer to attain its most stable conformation, which is a prerequisite condition for its binding to target molecule. Subsequently, the anti-BPA aptamer solution was reduced in 2 mM TCEP for 1 h to cleave disulphide bonds. For aptamer immobilisation, the GNPs/GR modified GCE was kept in a solution containing various concentrations of anti-BPA and MCH for 16 h at 4 °C in a 100% moisture-saturated environment. Finally, the anti-BPA/MCH/GNPs/GR/GCE was rinsed with deionised water, followed by drying under N<sub>2</sub> stream. The resulting electrode was then employed as the aptasensor in this work.

### 2.4. Electroanalytical measurements

The formation of anti-BPA and target complexes was performed by immersing the anti-BPA/MCH/GNPs/GR/GCE into binding buffer (25 mM Tris–HCl, pH 8.0 with 100 mM NaCl, 10 mM MgCl<sub>2</sub>, 25 mM KCl) containing a given BPA concentration for 30 min at room temperature, followed by thoroughly washing with binding buffer to remove unbound BPA. All electrochemical measurements were performed in 5.0 mM K<sub>3</sub>[Fe(CN)<sub>6</sub>]/K<sub>4</sub>[Fe(CN)<sub>6</sub>] containing 0.1 M KCl solution. Cyclic voltammetric (CV) measurements were

performed over a potential range from  $-0.1$  to  $+0.6$  V at a scan rate of  $50 \text{ mV s}^{-1}$ . The electrochemical differential pulse voltammetry (DPV) measurements were carried out under the following conditions: The voltage scanned from  $-0.1$  to  $+0.7$  V with a pulse height of  $50 \text{ mV}$ , the step height and the frequency were kept as  $50 \text{ mV}$  and  $5.0 \text{ Hz}$ , respectively.

The electrochemical data analysis was carried out and the decreasing percent of anodic peak currents before and after the sample treatment ( $\Delta I = (I_0 - I_1)/I_0 \times 100\%$ ) was measured. Where  $\Delta I$  is relative current change,  $I_0$  and  $I_1$  represent the anodic peak current before and after BPA treatment, respectively. Each sample was tested five times for the detection of BPA. The values obtained were the average of five results. All measurements were carried out at room temperature.

## 2.5. Sample preparation and procedures

The milk samples, including fresh liquid milk and milk powder, were purchased from a local supermarket (Hangzhou, China). The fresh liquid milk samples were prepared as the follows:  $5.0 \text{ mL}$  of liquid milk was first mixed with  $20 \text{ mL}$  Tris-HCl buffer solution. After  $15 \text{ min}$  sonication and  $10 \text{ min}$  shaking, the mixture was centrifuged for  $10 \text{ min}$ , and then supernatant was filtrated (Millipore Express PLUS Membrane Filter; pore size,  $0.22 \mu\text{m}$ ; filter diameter,  $25 \text{ mm}$ ). Next the filtrate was collected and added into  $25 \text{ mL}$  volumetric flask, diluted with Tris-HCl buffer solution to the calibration line. Finally, the obtained liquid milk sample was spiked with certain amounts of BPA standard solution. The preparation of the milk powder sample was similar to the above processes except that  $5.0 \text{ g}$  of milk powder was mixed with  $40 \text{ mL}$  of Tris-HCl buffer solution and the filtrate was collected in a  $50 \text{ mL}$  volumetric flask. The samples without adding BPA were used as negative control.

## 3. Results and discussion

### 3.1. Design strategy of the aptasensor

Fig. 1 schematically depicts the mechanism of the strategy in this work to fabricate the electrochemical aptasensor. The anti-BPA aptamer comprising 63 nucleotides that were covalently grafted on the GCE surface formed a cluster of long spacer arms on the substrate, leaving long tunnels for the redox probe ( $[\text{Fe}(\text{CN})_6]^{3-/4-}$ ) to reach the electrode surface. Here in the designed strategy, the anti-BPA aptamers acted as gate of the long tunnels. In the absence of BPA, the anti-BPA aptamers were thought to remain unfolded and the gate remained opened (Fig. 1(A)), thereby allowing the passage of electrons to electrode surface. However, upon addition of BPA, the conformation of aptamer was changed to G-quadruplex structure that closed the entrance of long tunnels and subsequently gate was closed, resulting in the blockage of electron flow to electrode surface (Fig. 1(B)). In addition to physical hindrance caused by the anti-BPA aptamer gate to electron flow, the binding of BPA exposed the negatively charged back bone of the anti-BPA aptamer to redox probe, further increasing the repulsion to electron flow. The increasing concentrations of BPA increased the formation of closed aptamer gate and subsequently decreased the number of open tunnel, resulting in decreased electrochemical signal (Fig. 1(C) and (D)). In our designed strategy, two factors: aptamer gate formation and exposition of negative charged bone, contributed to enhance the sensitivity of the aptasensor by decreasing the electrochemical signal upon BPA binding (Hayat, Andreescu, & Marty, 2013). This proposed aptasensor offers advantage for label-free detection of small molecules, eliminating the size factor of molecule.

### 3.2. Characterisation of the aptasensor

#### 3.2.1. Electrochemical characterisation of the modified electrodes

The immobilisation of each functionalised layer on GCE surface was confirmed through CV measurements. CVs of different modified electrodes in  $5.0 \text{ mM}$   $[\text{Fe}(\text{CN})_6]^{3-/4-}$  solution were shown in Fig. 2. The bare GCE had obvious redox peak (Fig. 2(a)). The GR/GCE (Fig. 2(b)) exhibited larger current response than that of bare GCE, which ascribed to the fact that GR/GCE could significantly enhance the conductivity of the electrode, facilitating the electron-transfer. After the GR/GCE was modified with GNPs (Fig. 2(c)), the peak current further increased, demonstrating that this kind of nanocomposite materials could generate synergy on electrochemical properties. When the anti-BPA aptamer was immobilised on the electrode, a decreased redox peak current (Fig. 2(d)) was obtained. It was reasonable that aptamers modified on the electrode surface could block the electron transfer of redox probe.

#### 3.2.2. Characteristics of the SEM

Fig. 3(A) is the typical AFM images and height profiles of GO. The thickness of the GO sheet obtained is about  $1 \text{ nm}$ , which is consistent with previously reported thickness of GO sheets (Marcano et al., 2010). The SEM image of GR modified GCE surface was shown in Fig. 3(B). The surface morphology of GR/GCE was characterised by many rolling wrinkles arising from the flexibility of GR sheets. Fig. 3(C) was SEM image of the prepared GNPs/GR nanocomposites modified surface. From the image we can see that gold nanoparticles distributed uniformly on the GR/GCE surface. As GNPs/GR nanocomposite structure gave a high specific surface area, it was able to provide a large surface area for aptamer attachment. More importantly, the doped GNPs were expected to enhance electronic transmission rate.

### 3.3. Optimisation of experimental conditions for aptasensor

#### 3.3.1. Optimisation of aptamer/MCH concentration

To obtain the maximum sensitivity, the concentration of aptamer ( $0.1$ – $10 \mu\text{M}$ ) and MCH ( $0.5$ – $10 \mu\text{M}$ ) were optimised. The relative DPV peak current changes ( $\Delta I$ ) before and after BPA ( $1.0 \mu\text{M}$ ) addition were obtained with a fixed concentration of MCH ( $1.0 \mu\text{M}$ ) and different aptamer concentrations ( $0.1$ ,  $1.0$ ,  $2.0$ ,  $5.0$  and  $10 \mu\text{M}$ ) (Fig. 4(A)), and also with a fixed concentration of aptamer ( $1.0 \mu\text{M}$ ) and several concentrations of MCH ( $0.5$ ,  $1.0$ ,  $2.0$ ,  $5.0$  and  $10 \mu\text{M}$ ) (Fig. 4(B)). The best conditions for assays were determined according to the sensitivity (maximum  $\Delta I$ ) of the proposed aptasensor. Therefore, the aptamer concentration of  $1.0 \mu\text{M}$  and  $2.0 \mu\text{M}$  of MCH were adopted in this work.

#### 3.3.2. Optimisation of aptamer/MCH incubation time

The incubation time of aptamer/MCH on the GNPs/GR/GCE surface was also investigated to obtain a high sensitivity of the fabricated aptasensor. The dependence of incubation time on the DPV peak current response before and after BPA ( $1.0 \mu\text{M}$ ) addition was displayed in Fig. 4(C). The DPV peak current change ( $\Delta I$ ) increased with increasing incubation time and reached a plateau at  $12 \text{ h}$ , indicating that aptamer/MCH was saturated on the modified GCE surface. Thus,  $12 \text{ h}$  was chosen as the optimum incubation time.

#### 3.3.3. Optimisation of BPA detection time

Beside the effect of aptamer/MCH concentration and incubation time, it was found that a different detection time of BPA caused a visible difference on the DPV peak current change ( $\Delta I$ ). Therefore, the dependence of BPA detection time on the increase of  $\Delta I$  was studied to determine the optimum detection time of BPA. As

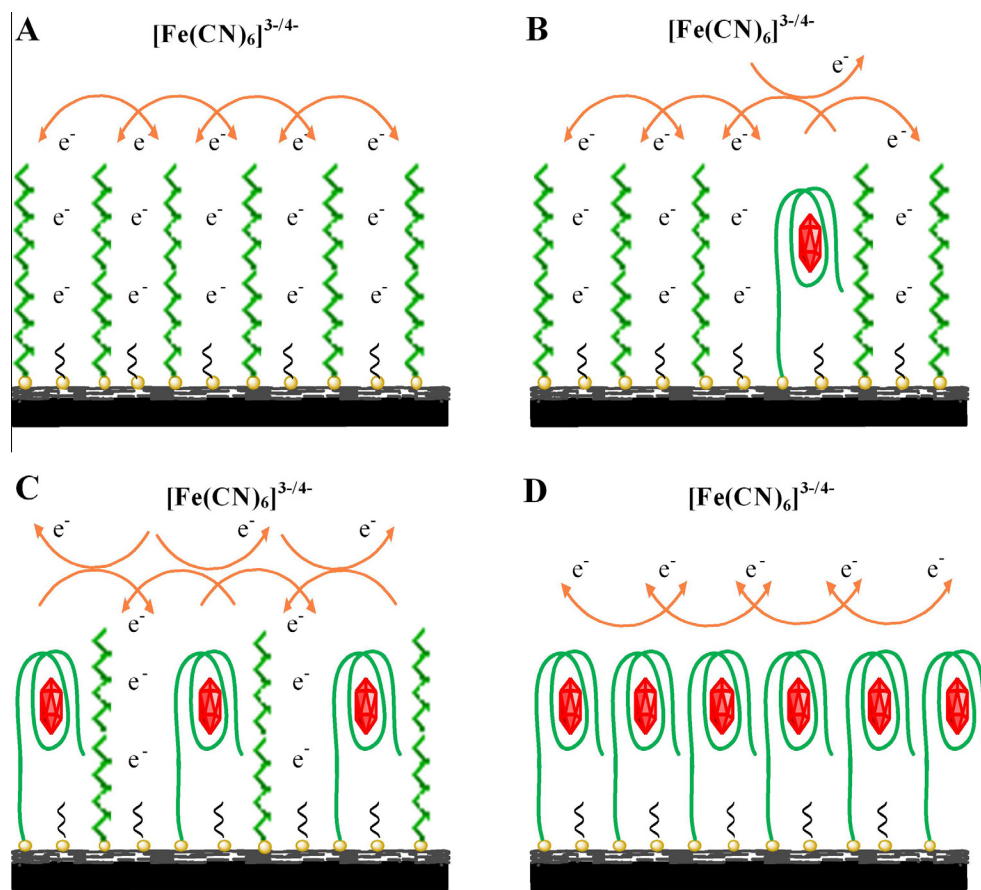


**Fig. 1.** Schematic illustration of the designed strategy for the determination of BPA; the tunnel gates remain open in the absence of BPA (A); addition of BPA (lower concentration) results in closing of some of the gates, due to aptamer conformational changes (B); increase of BPA further increase the number of closed gates (C) and at higher concentration almost all the gates get closed (D).

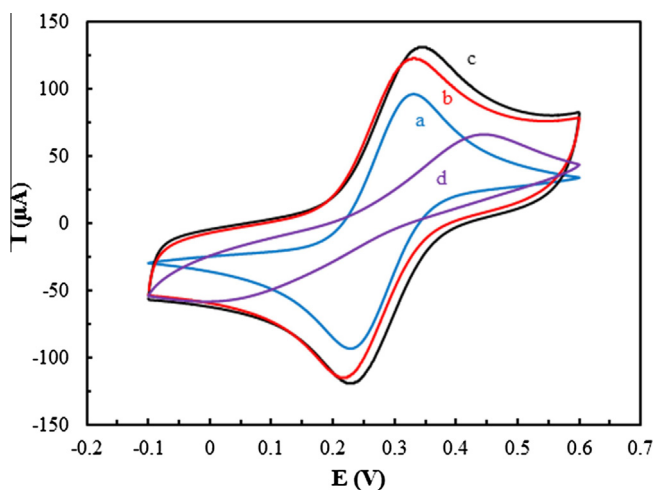


**Fig. 2.** CV of the bare GCE (a), GR/GCE (b), GNPs/GR/GCE (c), anti-BPA/GNPs/GR/GCE (d) in aqueous solution consisting of 5.0 mM  $[\text{Fe}(\text{CN})_6]^{3-/4-}$  and 0.1 M KCl. The voltage range:  $-0.1$  to  $+0.6$  V; scan rate:  $50 \text{ mV s}^{-1}$ .

shown in Fig. 4(D),  $\Delta I$  increased immediately when BPA ( $1.0 \mu\text{M}$ ) was introduced and then tended to stabilise after 30 min, indicated that the aptamer/BPA complexes were saturated onto the electrode surface. Thus, 30 min was selected as the BPA detection time.

### 3.4. Performance of the aptasensor

#### 3.4.1. Calibration curve of the aptasensor

The aptasensors were incubated with different concentrations of BPA under the optimal conditions and the DPV responses of the proposed aptasensor were recorded. As seen in Fig. 5(A), it displayed that the DPV peak current decreased with the increasing concentrations of BPA in the range from  $0 \mu\text{M}$  to  $10 \mu\text{M}$ . In addition, a linear calibration curve was obtained for BPA detection between  $0.01 \mu\text{M}$  and  $10 \mu\text{M}$  (Fig. 5(B)) and the correlation coefficient ( $R^2$ ) was 0.9924. The limit of detection was  $0.005 \mu\text{M}$  ( $S/N = 3$ ). From Fig. 5(B), changes in the current ( $\Delta I$ ) were about 10–45% when the BPA concentration was between  $0.01 \mu\text{M}$  and  $100 \mu\text{M}$ . Although lower concentrations ( $0.0001 \mu\text{M}$  and  $0.001 \mu\text{M}$ ) caused a decreased current (about 5%), this may be not due to the binding of BPA to the aptamer since the background signal change was also about 5%. One possible explanation for the background signal of the aptasensor was the non-specific adsorption caused by the high concentration of binding buffer on the electrode surface (Kim et al., 2007). At the treatment of  $100 \mu\text{M}$  BPA, the current change was almost the same as that of  $10 \mu\text{M}$  BPA. It might be possible that  $1 \mu\text{M}$  of anti-BPA aptamer immobilised on the modified electrode surface was saturated by more than  $10 \mu\text{M}$  of BPA.

#### 3.4.2. Specificity of the aptasensor

From the practical point, not only does an aptasensor have to be sensitive to different concentrations of the analyte, but also it must



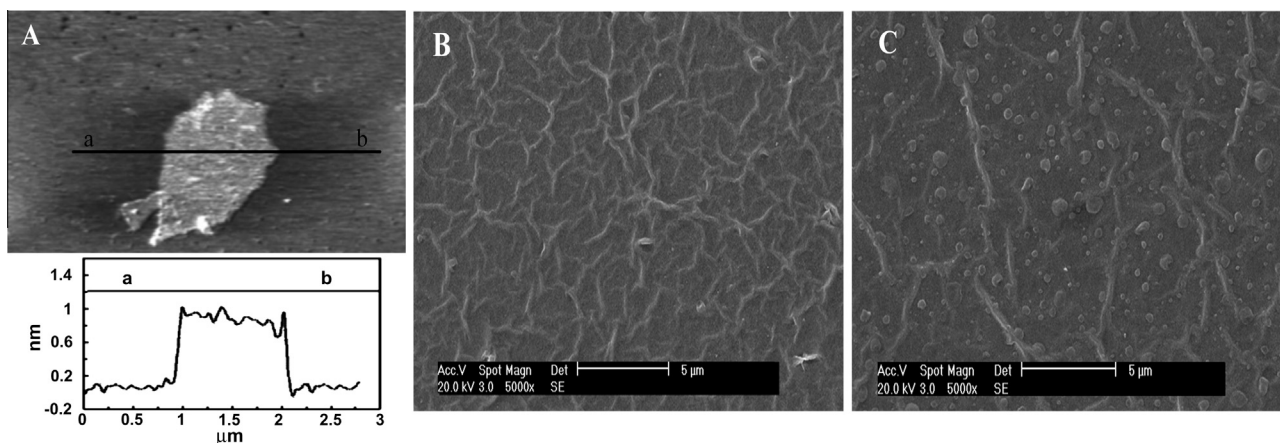


Fig. 3. AFM image of GO sheet (A). SEM images of the working surface area of bare GCE after GR modified (B) and after GNPs/GR modified (C).

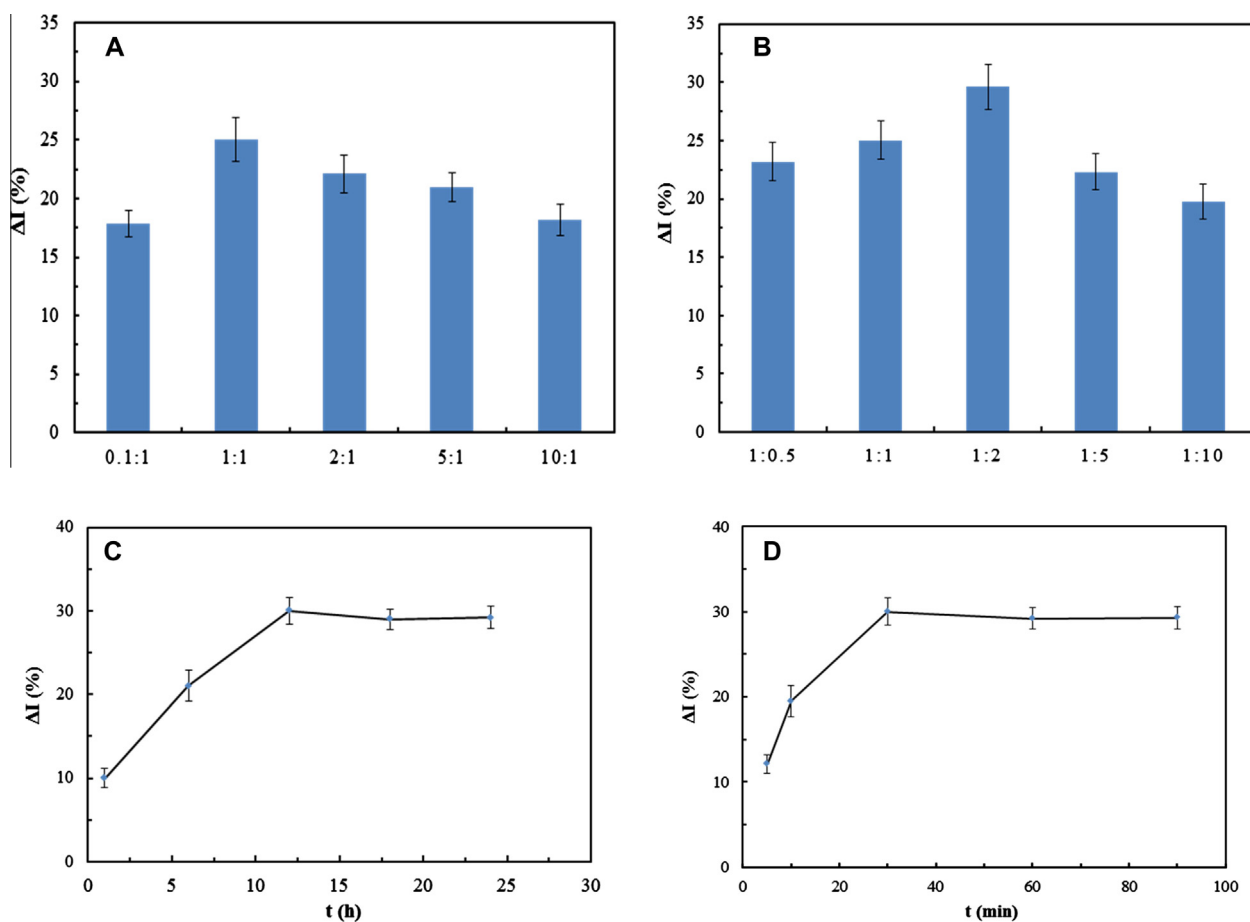


Fig. 4. Relative DPV peak current change ( $\Delta I$ ) obtained during optimisation of aptamer/MCH (A and B), aptamer/MCH incubation time (C) and BPA detection time (D). The immobilised MCH concentration was 1.0  $\mu\text{M}$  and the five plots corresponding to assays with 0.1, 1.0, 2.0, 5.0 and 10  $\mu\text{M}$  of aptamer (A). Using 1.0  $\mu\text{M}$  aptamer for immobilisation step, the results came from the MCH concentrations of 0.5, 1.0, 2.0, 5.0 and 10  $\mu\text{M}$  (B). Error bars show the standard deviations of measurements taken from five tests.

be specific. The specificity of the proposed aptasensor was also examined by detecting the DPV peak current change ( $\Delta I$ ) in the presence of BPA and three interfering agents: BPB, BP and 6F-BPA. The experimental results were shown in Fig. 5(C). It was found that only 1  $\mu\text{M}$  of BPA gave significant peak current change, while the same concentration of the other three interfering agents had slight emissions. The above results confirmed that there was insignificant cross reactivity for BPA analogues and the

developed aptasensor could be used to determinate BPA with high specificity.

#### 3.4.3. Reproducibility and stability of the aptasensor

A long-time stability of the aptasensor was studied on a 14-day period. After keeping it in refrigerator (4  $^{\circ}\text{C}$ ) for 2 weeks, the aptasensor was used to detect the same BPA concentration (1  $\mu\text{M}$ ). The current change ( $\Delta I$ ) was 30% before and 26% later. It did not show

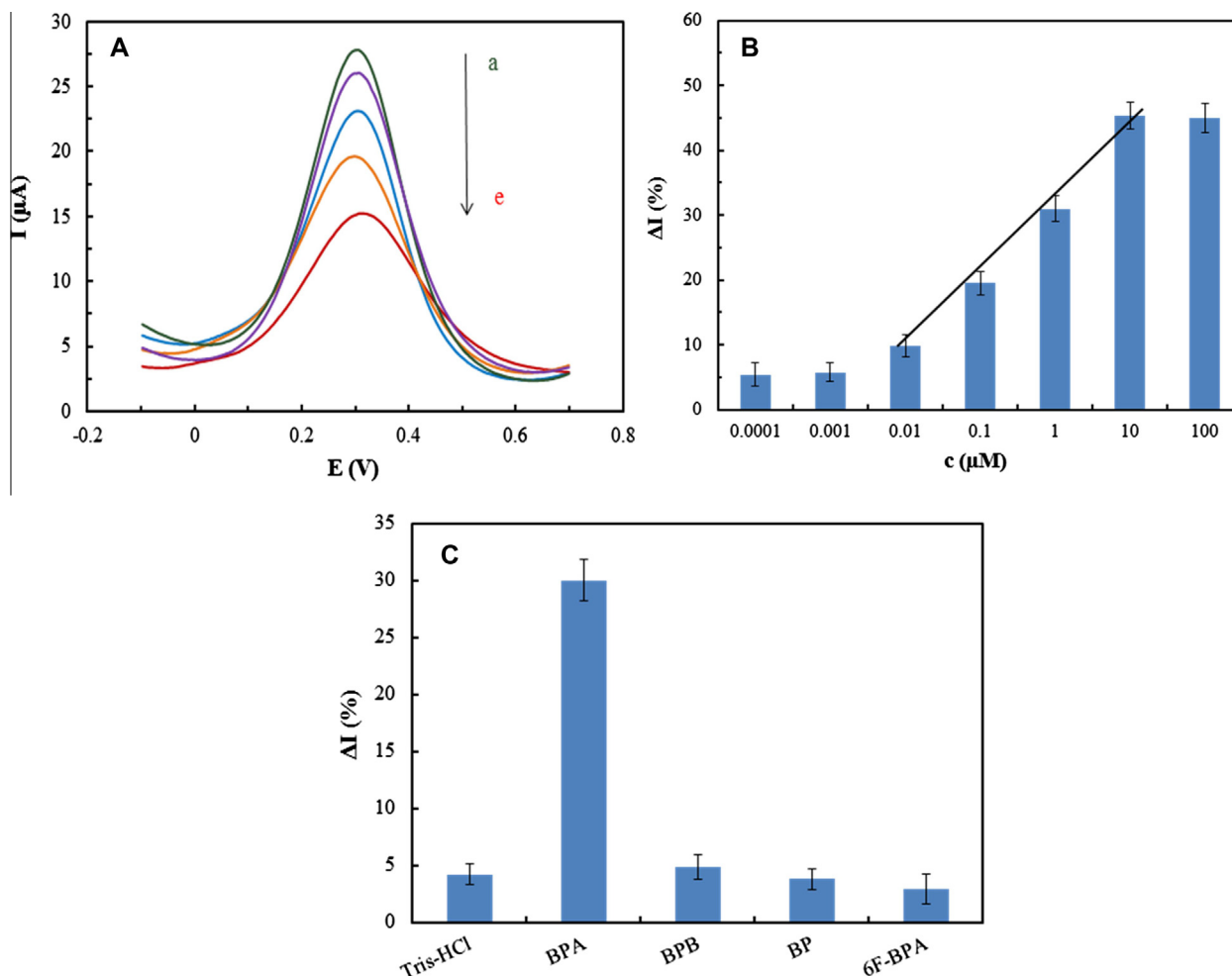


**Fig. 5.** DPV curves of the aptasensor incubated with different concentrations of BPA (a–e: the concentrations of BPA are 0, 0.01, 0.1, 1.0 and 10  $\mu\text{M}$ ) (A). Linear relationship between the peak current change ( $\Delta I$ ) and the concentrations of BPA (B). Specificity of the aptasensor to 1.0  $\mu\text{M}$  BPA by comparing it to the interfering agents, including BPB, BP and 6F-BPA (C). Error bars show the standard deviations of measurements taken from five tests.

an obvious change (lower than 5%), demonstrating that the aptasensor had good stability.

The reproducibility of the aptasensor was examined by testing each sample (1  $\mu\text{M}$  of BPA) with five times. The resulting relative standard deviation (RSD) was 3.2% for five determinations by independently prepared aptasensor. The experimental results indicated good reproducibility of the fabrication protocol.

#### 3.4.4. Preliminary application of the aptasensor

The feasibility of the proposed aptasensor for use in measuring BPA in food samples was investigated. Two milk samples, including liquid milk and milk powder, were employed. The values in Table 1 were obtained by the DPV response against certain amounts of BPA

in milk samples. As seen in Table 1, the existing milk samples in market were free of BPA. In addition, the average recovery was about 105% and the RSD was less than 5.2%. Compared with the RSD of the proposed aptasensor in the determination of BPA in Tris–HCl solution, the RSD of real assays were a little larger due to the presence of interferences in spiked milk samples. However, the prepared aptasensor showed comparable performance compared with other aptasensors in real assays (Liu et al., 2011 and Cao et al., 2009), indicated that the developed aptasensor could be applied for the analysis of BPA in milk samples.

## 4. Conclusion

A label-free electrochemical aptasensor for the determination of BPA was developed. The aptamer was directly immobilised on the GNPs/GR nanocomposite film modified electrode as a BPA capture. Binding of BPA caused current to decrease, thus providing a basis for detection. Compared to the existing electrochemical aptasensors for BPA detection based on target induced conformational changes, our designed aptasensing platform provided reduced complexity of the system. In addition, as the aptamer gate formation and back bone charge exposition upon BPA binding is involved to get electrochemical signal, eliminating the size factor of molecule for label-free detection. More importantly, the proposed aptasensor was applied successfully to the determination of BPA in

**Table 1**  
Recoveries of BPA from spiked milk samples ( $n = 5$ ).

Sample	Added ( $\mu\text{M}$ )	Found ( $\mu\text{M}$ )	Recovery (%)	RSD (%)
Liquid milk	0	0	–	1.8
	0.1	0.11	110	3.5
	0.5	0.58	116	3.2
	1.0	0.96	96	4.8
Milk powder	0	0	–	2.1
	0.1	0.09	90	4.2
	0.5	0.53	106	3.9
	1.0	1.12	112	5.2

milk products, and the average recovery was about 105%. Therefore, this designed aptasensor was expected to have a potential application in food inspection.

### Acknowledgement

The authors gratefully acknowledge the financial support provided by National Natural Science Foundation of China (31201367).

### Appendix A. Supplementary data

Supplementary data associated with this article can be found, in the online version, at <http://dx.doi.org/10.1016/j.foodchem.2014.04.058>.

### References

- Al-Mashat, L., Shin, K., Kalantar-zadeh, K., Plessis, J. D., Han, S. H., Kojima, R. W., et al. (2010). Graphene/polyaniline nanocomposite for hydrogen sensing. *Journal of Physical Chemistry C*, *114*(39), 16168–16173.
- Bang, G. S., Cho, S., & Kim, B. G. (2005). A novel electrochemical detection method for aptamer biosensors. *Biosensors and Bioelectronics*, *21*(6), 863–870.
- Cao, Q., Zhao, H., Zeng, L. X., Wang, J., Wang, R., Qiu, X. H., et al. (2009). Electrochemical determination of melamine using oligonucleotides modified gold electrodes. *Talanta*, *80*(2), 484–488.
- Chambasha, B., & Lee, H. K. (2004). Analysis of endocrine disrupting alkylphenols, chlorophenols and bisphenol-A using hollow fiber-protected liquid-phase microextraction coupled with injection port-derivatization gas chromatography–mass spectrometry. *Journal of Chromatography A*, *1057*(1–2), 163–169.
- Ellington, A., & Szostak, J. W. (1990). In vitro selection of RNA molecules that bind specific ligands. *Nature*, *346*(6287), 818–822.
- Hayat, A., Andreescu, S., & Marty, J. L. (2013). Design of PEG–aptamer two piece macromolecules as convenient and integrated sensing platform: Application to the label free detection of small size molecules. *Biosensors and Bioelectronics*, *45*(1), 168–173.
- Hiroi, H., Tsutsumi, O., Momoeda, M., Takai, Y., Osuga, Y., & Taketani, Y. (1999). Differential interactions of bisphenol A and 17 $\beta$ -estradiol with estrogen receptor  $\alpha$  (ER $\alpha$ ) and ER $\beta$ . *Endocrine Journal*, *46*(6), 773–778.
- Hong, W. J., Bai, H., Xu, Y. X., Yao, Z. Y., Gu, Z. Z., & Shi, G. Q. (2010). Preparation of gold nanoparticle/graphene composites with controlled weight contents and their application in biosensors. *Journal of Physical Chemistry C*, *114*(4), 1822–1826.
- Huang, C., Huang, Y., Cao, Z., Tan, W., & Chang, H. (2005). Aptamer-modified gold nanoparticles for colorimetric determination of platelet-derived growth factors and their receptors. *Analytical Chemistry*, *77*(17), 5735–5741.
- Inoue, K., Kato, K., Yoshimura, Y., Makino, T., & Nzkazawa, H. (2000). Determination of bisphenol A in human serum by high-performance liquid chromatography with multi-electrode electrochemical detection. *Journal of Chromatography B*, *749*(1), 17–23.
- Jo, M. J., Lee, J. A., Lee, S., Hong, S. W., Yoo, J. W., Kang, J., et al. (2011). Development of single-stranded DNA aptamers for specific bisphenol A detection. *Oligonucleotides*, *21*(2), 85–91.
- Kim, Y. S., Jung, H. S., Matsuura, T., Lee, H. Y., Kawai, T., & Gu, M. B. (2007). Electrochemical detection of 17 $\beta$ -estradiol using DNA aptamer immobilized gold electrode chip. *Biosensors and Bioelectronics*, *22*(11), 2525–2531.
- Le, H. H., Carlson, E. M., Chua, J. P., & Belcher, S. M. (2008). Bisphenol A is released from polycarbonate drinking bottles and mimics the neurotoxic actions of estrogen in developing cerebellar neurons. *Toxicology Letters*, *176*(2), 149–156.
- Li, R. Y., Xia, Q. F., Li, Z. J., Sun, X. L., & Liu, J. K. (2013). Electrochemical immunosensor for ultrasensitive detection of microcystin-LR based on graphene–gold nanocomposite/functional conducting polymer/gold nanoparticle/ionic liquid composite film with electrodeposition. *Biosensors and Bioelectronics*, *44*(1), 235–240.
- Liu, S., Xing, X. R., Yu, J. H., Lian, W. J., Li, J., Cui, M., et al. (2011). A novel label-free electrochemical aptasensor based on graphene–polyaniline composite film for dopamine determination. *Biosensors and Bioelectronics*, *36*(1), 186–191.
- Marcano, D. C., Kosynkin, D. V., Berlin, J. M., Sinitzki, A., Sun, Z. Z., Slesarev, A., et al. (2010). Improved synthesis of graphene oxide. *ACS Nano*, *4*(8), 4806–4814.
- Marchesini, G. R., Meulenberg, E., Haasnoot, W., & Irth, H. (2005). Biosensor immunoassays for the detection of bisphenol A. *Analytica Chimica Acta*, *528*(1), 37–45.
- Moreno, M. J., D'Arienzo, P., Manclus, J. J., & Montoya, A. (2011). Development of monoclonal antibody-based immunoassays for the analysis of bisphenol A in canned vegetables. *Journal of Environmental Science and Health Part B-Pesticides Food Contaminants and Agricultural Wastes*, *46*(6), 507–509.
- Ohkuma, H., Abe, K., Ito, M., Kokado, A., Kambegawa, A., & Maeda, M. (2002). Development of a highly sensitive enzyme-linked immunosorbent assay for bisphenol A in serum. *Analyst*, *127*(1), 93–97.
- Palanza, P., Gioiosa, L., vom Saal, F. S., & Parmigiani, S. (2008). Effects of developmental exposure to bisphenol A on brain and behavior in mice. *Environmental Research*, *108*(2), 150–157.
- Safe, S. H. (2000). Endocrine disruptors and human health—is there a problem? An update. *Environmental Health Perspectives*, *108*(6), 487–493.
- Sato, Y., Kondo, Y., Tsujita, K., & Kawai, N. (2005). Degradation behavior and recovery of bisphenol-A from epoxy resin and polycarbonate resin by liquid-phase chemical recycling. *Polymer Degradation and Stability*, *89*(2), 317–326.
- Stojanovic, M. N., & Landry, D. W. (2002). Aptamer-based colorimetric probe for cocaine. *Journal of the American Chemical Society*, *124*(33), 9678–9679.
- Tuerk, C., & Gold, L. (1990). Systematic evolution of ligands by exponential enrichment: RNA ligands to bacteriophage T4 DNA polymerase. *Science*, *249*(4968), 505–510.
- Wang, F. R., Yang, J. Q., & Wu, K. B. (2009). Mesoporous silica-based electrochemical sensor for sensitive determination of environmental hormone bisphenol A. *Analytica Chimica Acta*, *638*(1), 23–28.
- Watabe, Y., Kondo, T., Morita, M., Tanaka, N., Haginaka, J., & Hosoya, K. (2004). Determination of bisphenol A in environmental water at ultra-low level by high-performance liquid chromatography with an effective on-line pretreatment device. *Journal of Chromatography A*, *1032*(1–2), 45–49.
- Wilson, D. S., & Szostak, J. W. (1999). In vitro selection of functional nucleic acids. *Annual Review of Biochemistry*, *68*(1), 611–647.
- Yin, H. S., Cui, L., Chen, Q. P., Shi, W. J., Ai, S. H., Zhu, L. S., et al. (2011). Amperometric determination of bisphenol A in milk using PAMAM–Fe<sub>3</sub>O<sub>4</sub> modified glassy carbon electrode. *Food Chemistry*, *125*(3), 1097–1103.
- Zafra-Gómez, A., Ballesteros, O., Navalón, A., & Vilchez, J. L. (2008). Determination of some endocrine disrupter chemicals in urban wastewater samples using liquid chromatography–mass spectrometry. *Microchemical Journal*, *88*(1), 87–94.
- Zhao, M. P., Li, Y. Z., Guo, Z. Q., Zhang, X. X., & Chang, W. B. (2002). A new competitive enzyme-linked immunosorbent assay (ELISA) for determination of estrogenic bisphenols. *Talanta*, *57*(6), 1205–1210.